Journal of Nuclear Materials 85 & 86 (1979) 547–552

VOID GROWTH CHARACTERISTICS IN LASER FUSION REACTOR FIRST WALLS

N. M. GHONIEM and G. L. KULCINSKI

UCLA and University of Wisconsin

The damaging effects of microexplosion products on void behavior in unprotected stainless steel laser fusion first walls are analyzed using the Dynamic Rate Theory. The preliminary results from this work indicate that in the zones where the temperature excursions are the highest, gas bubbles will be the predominant defect and the dislocation loops and voids will be annealed out. As one moves farther into the first wall, the growth or shrinkage of voids depends on the ambient temperature and the magnitude of the displacement rate.

1. INTRODUCTION

One of the most unique features of proposed laser fusion reactors is the pulsed nature of the energy release [1-3]. As a result of laser initiated implosions, the thermonuclear burn takes place over tens of picoseconds, releasing a large variety of energetic ions, neutrons, and photons. If the first walls of the reaction chamber are unprotected, this radiation can strike the walls over times ranging from 10^{-8} to 10^{-5} seconds. Such damage rates can cause significant thermal transients ($\sim$1000°C or more) and high displacement rates (10-100 dpa/s). The distances over which this energy is deposited varies from a few thousand angstroms in the case of reflected laser light to several microns for the charged particle debris (D^+, T^+, He^{++}, and pellet material such as carbon, iron, etc.), up to millimeters for high energy X-rays and 10's of centimeters for neutrons. Hence, it appears that there will be several distinct zones of damage in the first wall which will have to be analyzed separately to determine the ultimate response of the wall to the pulsed radiation fields.

Previous analyses have treated the temporal and spatial response of Cu [4], Mo and C [5] and 316 SS [6] first walls to a general pellet spectra which may be typical of a 100 MJ yield. Theories have also been developed to treat rapidly changing damage conditions as they might affect the growth and shrinkage of voids in metals [7]. The object of this paper is to combine the two previous lines of research so that we might gain some insight as to the behavior of voids in each of the various damage zones.

2. CALCULATIONAL MODEL

Because of the complex nature of the temperature and displacement transients, it is necessary to make several simplifying assumptions before proceeding with the calculations. The major assumptions are listed below.

- There is no mechanism to protect the first wall from the wave of pellet debris and reaction products.
- We assume that before the first pulse of radiation arrives, the first wall has a uniform microstructure consisting of 1.4×10^{13} interstitial dislocation loops per cm^3, 20.5 Å in radius, and 1.1×10^{12} voids per cm^3, 20 Å in radium. The densities are typical of 316 SS irradiated in EBR-II to 0.5 dpa at 500°C [8]. It has to be born in mind that such low defect densities are indicative of a microstructure in the process of nucleation. However, we recognize that a more detailed treatment of nucleation of defects during pulsed irradiation is needed.
- The voids are assumed to each contain 50 atoms of inert gas which will support an equilibrium bubble size of 10 Å in radius.

The first wall was divided up into four zones as described in Figure 1. The first zone represents the region where the charged particle debris is stopped (first few microns) and hence has the highest thermal transients and displacement rates. The second zone (up to $\sim$5 microns) is similar to the first but somewhat deeper into the solid where the thermal pulses are important but the only displacement rate is due to neutrons. The third zone represents the region ($\sim$5-20 microns) which can experience modest ($\sim$100°C) thermal pulses and neutron damage. Finally, the fourth zone represents the rest of the solid which experiences pulsed damage from neutrons, but remains at the ambient temperature (assumed to be 500°C in this case).

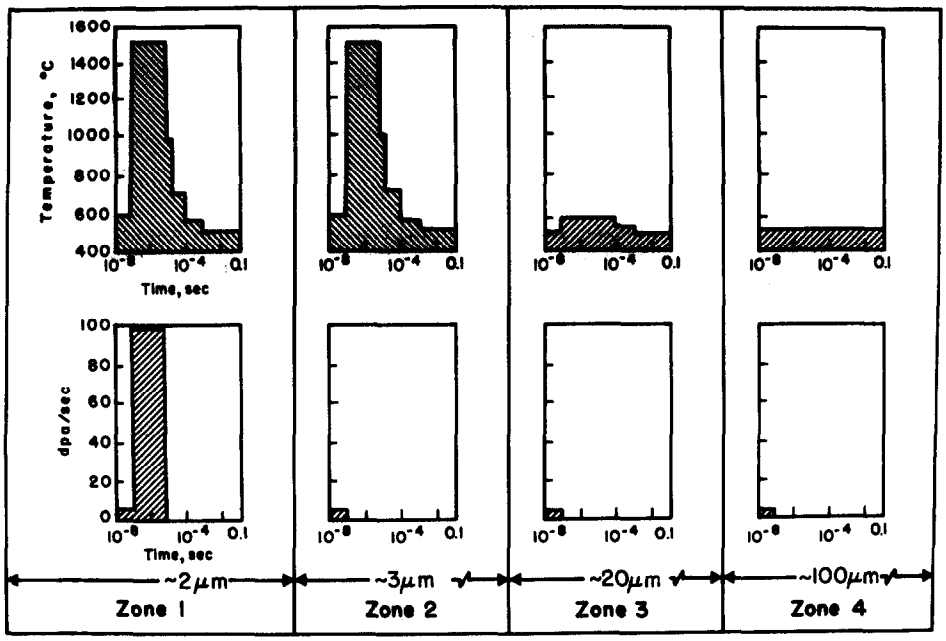

Fig. 1. Temperature and displacement rate profiles at various depths of the first wall resulting from a single microexplosion.

• The equations and materials parameters for 316 SS which describe the time behavior of the defect structure and void growth/annealing kinetics are taken from the Fully Dynamic Rate Theory (FDRT) described elsewhere [7].
• No account has been made for spatial point defect diffusion from one zone to the other in the manner proposed by Mansur and Yoo [9]. This is an improvement which will be examined in the future.
• The temperature pulses and displacement rates in 316 SS are taken from work by McCarville, et al. [6], and idealized in the manner illustrated in Figure 1 and listed in Table 1 for case of calculation.

The results reported in this paper are organized as follows: first, the effect of a single pulse of radiation on the microstructure in a pre-irradiated first wall is analyzed in detail for zone 1. Next, the variations in cavity and loop radii for zones 2, 3 and 4 are presented. This is followed by a brief discussion of the effects of ten consecutive pulses, spaced 0.1 of a second apart. Finally, the effect of different initial void radii on the final microstructure is investigated.

3. RESULTS AND DISCUSSION

3.1 Near Surface Region (Zone 1)

This zone is characterized by high temperature and displacement rates as discussed previously. Figure 2 shows that vacancy and interstitial concentrations increase linearly during the neutron damage, at least up to 10^{-7} seconds. One can notice that C_v is slightly lower than C_i in this time domain because of the direct formation of vacancy loops. Between 0.1 microsecond and 5 microseconds, the displacement rate is very high (100 dpa/s) which maintains relatively high concentrations of both vacancies and interstitials. It is important to observe that the vacancy concentration is only slightly above its thermal equilibrium value (C_v^e). Immediately after the damage pulse ceases, the interstitial concentration decreases sharply because of the high interstitial diffusion coefficient. On the other hand, the vacancy concentration remains constant up to about 10^{-3} seconds before it decreases due to vacancy absorption into vacancy loops.

Fluxes for void growth ($\phi_v^e = D_v C_v$), shrinkage (due to interstitial absorption; $\phi^i = D_i C_i$, and vacancy emission; $\phi_v^e = D_v C_v^e \exp\{((2\gamma/R) - p) \Omega/kT\}$ are plotted on Figure 3 as functions of irradiation time. Up to 0.1 μ seconds, the interstitial flux arriving at voids (ϕ^i) is appreciably larger than the incoming vacancy flux (ϕ^v) causing the void to shrink. However, due to the very short time during which this occurs, the average void and loop radii are only slightly reduced, as can be seen from Figure 4. During the remaining part of the irradiation pulse, the vacancy flux is always larger than the flux of interstitials. However, due to the high temperature between 0.1 and

Table 1

Damage Conditions Assumed for This Study

	Temperature, °C				Displacement Rate, dpa/s			
	Zone Number				Zone Number			
Time	1	2	3	4	1	2	3	4
0-0.1 μs	600	600	500	500	5	5	5	5
0.1-5 μs	1500	1500	600	500	100	0	0	0
5-10 μs	1000	1000	600	500	0	0	0	0
10-100 μs	700	700	600	500	0	0	0	0
100-1000 μs	570	570	550	500	0	0	0	0
1 ms - 0.1 sec	500	500	500	500	0	0	0	0

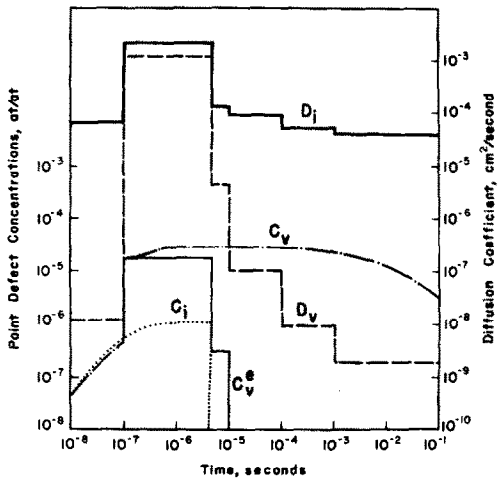

Fig. 2. Point defect concentrations and diffusion coefficients as functions of time (Zone 1).

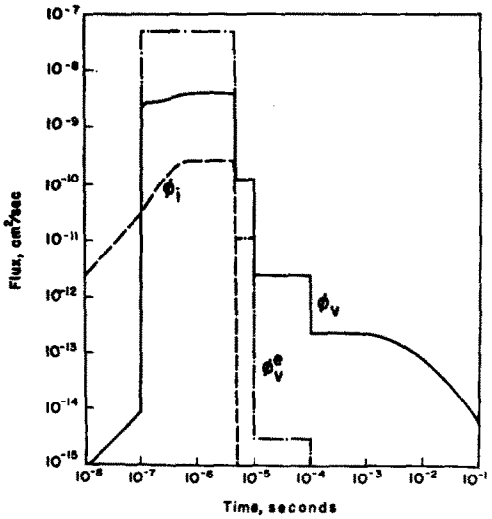

Fig. 3. Point defect fluxes as functions of time (Zone 1).

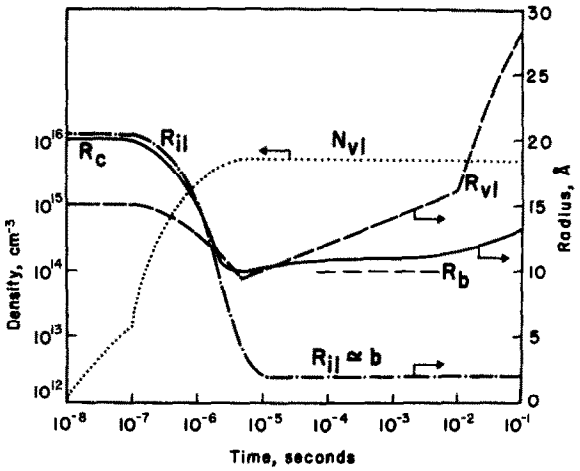

Fig. 4. Microstructure components for a single irradiation pulse in Zone 1.

5 μ seconds, the emission flux from the surface of voids (ϕ_v^e) is much larger than ($\phi^v - \phi^i$), thus the void again shrinks. This high temperature also anneals out all interstitial loops. (The average radius, R_{il}, shrinks down to ∿ one Burger's vector, b). Vacancy loops (R_{vl}) and voids (R_c) shrink to smaller sizes as well. Since an average void is assumed to contain 50 gas atoms, the void cannot shrink below the corresponding equilibrium bubble radius (R_b) of 10 Å. The high level of vacancy concentration achieved during the second period of the pulse (0.1 - 5 μs) induces slow cavity growth and a faster rate of growth for vacancy loops, as demonstrated in Figure 4. Vacancy loops and cavities compete for the existing vacancy population, and, therefore, their growth is achieved at the expense of decreasing the free vacancy concentration. This behavior can be explained by comparing Figures 3 and 4 for irradiation times longer than 1 millisecond.

3.2 Bulk Regions (Zones 2, 3, and 4)

The only difference between zone 1 and zone 2 is the lack of the high displacement rate produced by the pellet debris. The high temperature between 0.1 - 5 μ seconds anneals out all the components of the microstructure except for the gas filled cavities. Interstitial as well as vacancy loops disappear entirely by the end of 5 μ seconds as can be observed from Figure 5. Because each cavity is assumed to contain 50 gas atoms, it does not shrink below the equilibrium bubble radius. Following this high temperature period, the cavity starts to grow slowly, but never reaching its original radius before the next pulse. However, the final cavity radius in zone 2 is larger than the corresponding radius in zone 1 at the end of one pulse (∿15 Å compared to ∿13 Å). This is expected because there is no other microstructural components to compete with cavities for existing vacancies in zone 2.

The response of the microstructure in zones 3 and 4 has been found to be about the same. Therefore, we will only discuss here the response of dislocation loops and voids to the temperature and neutron damage described in section 2 for zone 3. Up to 0.1 μs, the vacancy loop concentration, $N_{v\ell}$, builds up linearly to 1.18×10^{13} loops/cm^3. No other appreciable changes occur in the microstructure during this very short time. The fast diffusion of interstitials to dislocation loops and cavities causes the interstitial loops to expand, while the vacancy loops and cavities shrink, as can be seen from Figure 6. The number of vacancy loops decreases slightly to $\sim 1.1 \times 10^{13}$ loops/cm^3 at the end of the pulse. The high vacancy emission from the cavity surface offsets the incoming vacancy flux, and the cavity radius remains almost constant in the later parts of the pulse (> 1 ms) at a value lower than the initial radius. Successive

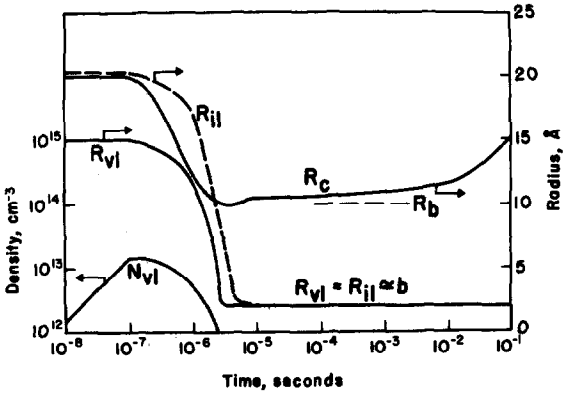

Fig. 5. Microstructure components for a single irradiation pulse in Zone 2.

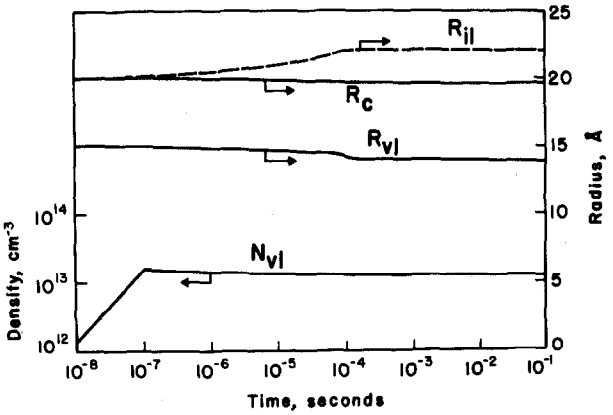

Fig. 6. Microstructure components for a single irradiation pulse in Zone 3.

pulses shrink the cavity further until it reaches the bubble equilibrium radius. It has to be recognized, however, that large initial cavity radii can lead to eventual growth of the cavities as will be explained in 3.3 below.

3.3 Train of Ten Pulses

The time dependence of cavities and vacancy loops due to a train of damage pulses in zone 1 is illustrated in Figure 7 for two different initial cavity radii. When the initial cavity radius (R_c^I) is 20 Å, it shrinks down to the bubble size (R_b = 10 Å) and then grows to ∿13 A at the end of the first pulse. On the other hand, vacancy loops expand to a radius of ∿28 Å at the end of the first pulse. Since the cavity shrinks down to the radius of an equilibrium bubble during the pulse, it grows to a final size which is controlled by the equilibrium bubble radius and not the initial void radius. Successive pulses will then result in cavity response identical to the first pulse. On the contrary, for larger initial cavity size (e.g. R_c^I = 50 Å), the behavior is quite different. Vacancy emission from the cavity surface is not very strong during the high temperature phase of the pulse, and, therefore, the cavity survives and actually grows slightly by the end of the first pulse. Cavity growth is accumulated with each pulse leading to void swelling rather than bubble swelling. It is apparent from this comparison that the gas content of the first zone will determine whether swelling will occur by the action of voids or bubbles.

3.4 The Effect of the Initial Cavity Size

The discussions in the previous sections indicated the importance of the initial cavity size in determining the final swelling behavior. The effect of the initial cavity radius on the final

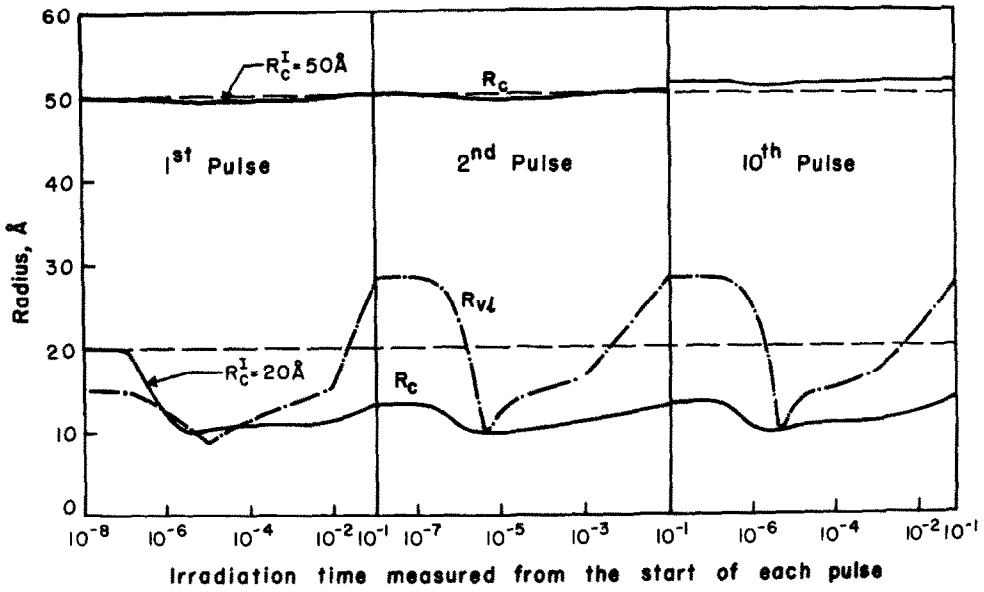

Fig. 7. The time dependence of the average cavity radiis (R_c) and the V-loop radius in a series of pulses.

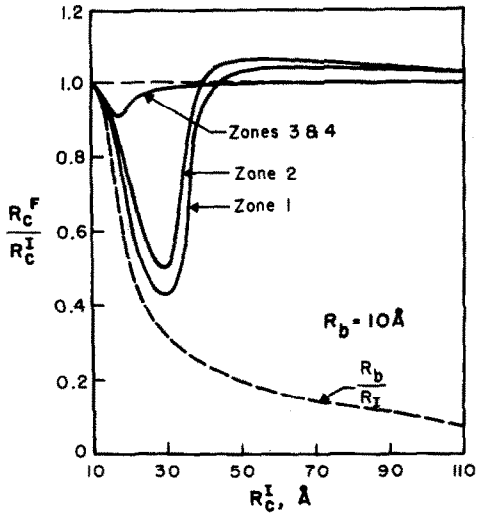

Fig. 8. The ratio (R_c^F/R_c^I) plotted as a function of initial cavity radius after ten pulses.

radius after ten pulses is summarized in Figure 8. The ratio of the final cavity radius to the initial cavity radius [R_c^F/R_c^I] is plotted as a function of the initial cavity radius.

When the cavity radius is close to the equilibrium bubble radius (10 Å in this case), the cavity shrinks because of the pulsed irradiation and the ratio [R_c^F/R_c^I] is less than unity. This is observed for all zones, as shown in Figure 8. It is interesting to note that above initial radii of 44 Å in zone 1 and ~40 Å in zone 2, cavities continue to grow with irradiation. However, the growth in zone 2 is larger than in zone 1, primarily due to the lack of surviving vacancy loops in zone 2. One can also notice from the same figure that the changes in the cavities of zone 3 and 4 are not very large because of the moderate temperature excursions and the very small amount of damage accompanying each pulse (5×10^{-7} dpa/pulse). For a complete discussion on the final swelling under conditions similar to zones 3 and 4, the reader is referred to the analysis of reference [10].

4. CONCLUSIONS

(1) The very high temperature pulse in the near surface region will override the high dpa rate due to the implanted species and cause the interstitial dislocation structure to anneal during each pulse. However, the high displacement rates produce significant vacancy loop concentrations which compete with voids for vacancies. This coupled with the large emission rates of voids at the high temperature will prohibit bubbles from exceeding their equilibrium size. Therefore, the behavior of this zone will be dominated by bubbles and vacancy loops, not voids.

(2) Since spatial zone 2 is deeper than where the debris is deposited but close enough to experience high temperature pulses, it will experience larger swelling than zone 1. The

reason for this behavior is that both the vacancy and interstitial loops anneal during the pulse and the excess vacancies can only add to the existing void structure.

(3) In the zones where there is little or no temperature increase and only neutron damage (e.g. zones 3 and 4), the dislocation structure is more important. The final swelling will depend on the initial void radius and ambient temperature. For high temperatures and small initial void size, the final swelling will be small. For low temperatures and large initial void size the swelling will be similar to that from steady-state irradiations.

(4) There is a critical void radius above which voids will grow and below which they will shrink to the equilibrium bubble size determined by the number of gas atoms contained. The critical void size is larger than that obtained from steady-state irradiations because of the high temperature transients associated with the thermonuclear burn.

One of the main features of this work is to point out the importance of the spatial and temporal damage conditions in an unprotected first wall for an Inertial Confinement Reactor. The analysis in this paper shows that there are at least three regions which could have drastically different microstructures after pulsed irradiation. These microstructures will undoubtedly effect mechanical properties and need to be investigated further.

ACKNOWLEDGEMENT

This work was partially supported by the Division of Laser Fusion, Department of Energy.

REFERENCES

[1] L. A. Booth, Central Station Power Generation by Laser Fusion, Los Alamos Report, LA-4858-NS, Vol. 1 (1972).

[2] J. Hovingh, J. A. Maniscalco, M. A. Peterson and R. W. Werner, "The Preliminary Design of a Suppressed-Ablation, Laser Induced Fusion Reactor," Proc. First Topical Meeting on the Tech. of Controlled Nuclear Fusion, CONF-740402-P1, San Diego, Ca., (1974) 96.

[3] G. L. Kulcinski, "The Newest Frontier in Radiation Damage Research --Laser Fusion Reactors", Univ. of Wisconsin Report, UWFDM-250 (1978).

[4] T.O. Hunter and G. L. Kulcinski, J. Nucl. Mat., 76/77 (1978) 383.

[5] T.O. Hunter, S. I. Abdel-Khalik and G. L. Kulcinski, Fusion Reactor Design Concepts, IAEA, Vienna, (1978) 561.

[6] T. McCarville, A. Hassanin and G. L. Kulcinski, "The Response of Stainless Steel to Pellet Debris in a Laser Fusion Reactor", University of Wisconsin Report, UWFDM-282 (1978).

[7] N. M. Ghoniem and G. L. Kulcinski. Rad. Effects, 39 (1978) 47.

[8] H. R. Brager and J. L. Straalsund. J. Nucl. Mat. 46 (1973) 134.

[9] L. K. Mansur and M. H. Yoo. J. Nucl. Mat. 74 (1978) 228.

[10] N. M. Ghoniem and G. L. Kulcinski. Nucl. Eng. and Design, 52 (1979) 111.